

Thermodynamic Assessment of Bio-Oriented Ti-Ta-Sn System

Lifang Yan ¹, Yingbiao Peng ^{1,2,3,*}, Tao Li ¹, Lianwu Yan ¹, Shiwen He ¹ and Tao Xu ²

¹ College of Metallurgical and Materials Engineering, Hunan University of Technology, Zhuzhou 412007, China; lifang_yan_hut@163.com (L.Y.); taoli_hut@163.com (T.L.); yanlianwu2008@126.com (L.Y.); hswcsu@126.com (S.H.)

² State Key Laboratory of Cemented Carbide, Zhuzhou Cemented Carbide Group Co., LTD., Zhuzhou 412000, China; xutao2005@126.com

³ State Key Laboratory for Powder Metallurgy, Central South University, Changsha 410083, China

* Correspondence: yingbiao-peng@csu.edu.cn; Fax: +86-0731-2218-3461

Abstract: The alloying elements Ta and Sn can effectively increase the stability of β -bcc phase, reduce Young's modulus and improve the shape-memory property of Ti-based biomedical alloys. The development of the thermodynamic database for Ti-based biomedical alloys promises thermodynamic predictions in composition design and process optimization. In this work, one key sub-ternary Ti-Ta-Sn system has been thermodynamically assessed based on critical evaluation of experimental phase equilibria. A self-consistent thermodynamic description for the Ti-Ta-Sn system including one ternary compound $Ti_{36}Ta_{28}Sn_{36}$ and six binary compounds considering the solubility of the third element has been obtained. Two isothermal sections at 973 and 1173 K and the liquidus projection have been calculated. Comparisons between the calculated and experimental phase equilibria validate the reliability of the present thermodynamic description. The influence of Ta and Sn contents on the transformation temperature and amount of α -hcp-Ti phase in β -bcc-(Ti,Ta) phase has been investigated based on thermodynamic calculations. The solidified phases in Ti-20Ta- x Sn ($x = 5, 15$ and 25 at.%) as-cast alloys have been thermodynamically calculated based on Scheil solidification simulations. The presently developed thermodynamic description of the Ti-Ta-Sn system would promote the establishment of multi-component Ti-based thermodynamic database and guide the development of Ti-based alloys.

Keywords: Ti-Ta-Sn ternary system; phase diagram; thermodynamic modeling; thermodynamic predictions



Citation: Yan, L.; Peng, Y.; Li, T.; Yan, L.; He, S.; Xu, T. Thermodynamic Assessment of Bio-Oriented Ti-Ta-Sn System. *Materials* **2021**, *14*, 1568. <https://doi.org/10.3390/ma14061568>

Academic Editor: Tomasz Czujko

Received: 9 February 2021

Accepted: 4 March 2021

Published: 23 March 2021

Publisher's Note: MDPI stays neutral with regard to jurisdictional claims in published maps and institutional affiliations.



Copyright: © 2021 by the authors. Licensee MDPI, Basel, Switzerland. This article is an open access article distributed under the terms and conditions of the Creative Commons Attribution (CC BY) license (<https://creativecommons.org/licenses/by/4.0/>).

1. Introduction

Metastable β -type Ti-based alloys have been widely used in biomedical applications because of their desirable properties such as similar Young's modulus to human bones, high strength, corrosion resistance behavior and good biocompatibility [1–3]. However, the presence of α'' martensite transformed from β during quenching or deformation significantly enlarges the elastic moduli difference between implant biomaterials and human bone [3]. In order to improve the biomedical properties of Ti-based alloys, alloying elements like Ta, Nb, Sn, Zr, Mo, etc have been reported to promise required properties [4–6]. It is reported that the alloying of Ta can effectively reduce the martensitic transformation temperature and thus stabilize β -bcc phase [2–5]. The third alloying element of Sn in Ti-Ta-based alloys can further adjust their properties, such as reducing elastic moduli, enhancing strength, improving corrosion resistance and so on [7,8]. To some extent, the mechanical properties of a material are related to its microstructure. As a result, it is of great importance to understand the thermodynamic behavior of the phases during the development of materials.

Generally, metastable β -bcc phase can be retained by rapid cooling. In order to obtain optimal combination of properties, Ti-based alloys composed with metastable β -bcc phase

can be subjected to aging treatment, and subsequently precipitating α _hcp phase [9,10]. For pure Ti, an allotropic transformation from β _bcc phase to α _hcp phase occurs at about 880 °C during cooling. For multicomponent Ti-based alloys, this transformation temperature strongly depends on alloy composition. Thus, an optimal combination of properties corresponding to the strengthening precipitates could be obtained through the design of alloying composition and aging heat treatment. CALPHAD technique has been proven to be a powerful tool to analysis phase stabilities and phase transformations [11], which can provide a strong theoretical basis to the development of Ti based alloys. However, the thermodynamic description of the Ti-Ta-Sn system has not been reported yet.

Hence, the present work aims to thermodynamically model the Ti-Ta-Sn system based on critical evaluation of experimental phase equilibria in the literature, to study the influence of Ta and Sn content on the phase transformation between α _hcp-Ti and β _bcc-(Ti,Ta) phases.

2. Experimental Information

The symbols denoting the phases in the Ti-Ta-Sn system and the crystal structure information are listed in Table 1 for facilitating reading.

Table 1. Crystal structure data of phases in the ternary system.

Phase	Designation	Prototype	Pearson Symbol	Space Group
α -Ti	hcp	Mg	hP2	P6 ₃ /mmc
β -Ti	bcc	W	cI2	Im3m
β -Ta	bcc	W	cI2	Im3m
Ti ₃ Sn	Ti ₃ Sn	Ni ₃ Sn	hP8	P4 ₁ 2 ₁ 2
β -Sn	bct	β -Sn	-	I4 ₁ /amd
α -Sn	diamond	C(diamond)	cF8	Fd3m
Ti ₂ Sn	Ti ₂ Sn	Ni ₂ In	hP6	P6 ₃ /mmc
Ti ₅ Sn ₃	Ti ₅ Sn ₃	Mn ₅ Si ₃	hP16	P6 ₃ /mcm
Ti ₆ Sn ₅	Ti ₆ Sn ₅	Ti ₆ Sn ₅	oI44	Immm
Ti ₂ Sn ₃	Ti ₂ Sn ₃	-	oC40	Cmca
Ta ₃ Sn	Ta ₃ Sn	Cr ₃ Si	cP8	Pm3n
Ta ₂ Sn ₃	Ta ₂ Sn ₃	CuMg ₂	oF48	Fddd

The literature information for the sub-binary systems have been critically reviewed in previous works [12–17], which will not be repeated here. The recent evaluations of the Ti-Ta [12], Ti-Sn [13] and Ta-Sn [14] binary systems are considered to be reliable and adopted in the present assessment of the Ti-Ta-Sn ternary system. Figure 1 shows the calculated phase diagrams of the Ti-Ta, Ti-Sn and Ta-Sn systems.

The major contribution to the phase diagram of the Ti-Ta-Sn system comes from the contributions by Wang et al. [16,17]. Using X-ray diffraction (XRD), scanning electron microscopy (SEM) and electron probe microanalysis (EPMA) techniques, the isothermal sections of the Ti-Ta-Sn ternary system were constructed based on 12 equilibrium alloys at 973 K [16] and 11 equilibrium alloys at 1173 K [17]. A total of four two-phase regions and three three-phase regions at 973 K, and five two-phase regions and two three-phase regions at 1173 K were experimentally detected [16,17]. One stoichiometric ternary compound was detected in the Ti-Ta-Sn system, Ti₃₆Ta₂₈Sn₃₆, at 1173 K [17]. No crystallographic information of Ti₃₆Ta₂₈Sn₃₆ has been reported in the literature. The sole study on this ternary compound was conducted by Wang et al. [17]. However, they only determined its composition using EPMA without further studying its crystal structure. Additionally, the solubility of the third element in boundary compounds were experimentally determined by means of EPMA technique [16,17]. The solubilities of Ta were determined to be 8.3 at.% at 973 K and 9.3 at.% at 1173 K in Ti₃Sn, no less than 8.8 at.% at 973 K and no less than 7.3 at.% at 1173 K in Ti₂Sn, about 4.2 at.% at 973 K and 6.1 at.% at 1173 K in Ti₅Sn₃, about 16.8 at.% at 973 K and no less than 15.5 at.% at 1173 K in Ti₆Sn₅, and no less than 15.8 at.%

at 973 K in Ti_2Sn_3 [16,17]. The EPMA results indicated that Ta mainly replaces Ti in all the Ti-Sn boundary compounds and Ti mainly replaces Ta in both Ta_3Sn and Ta_2Sn_3 .

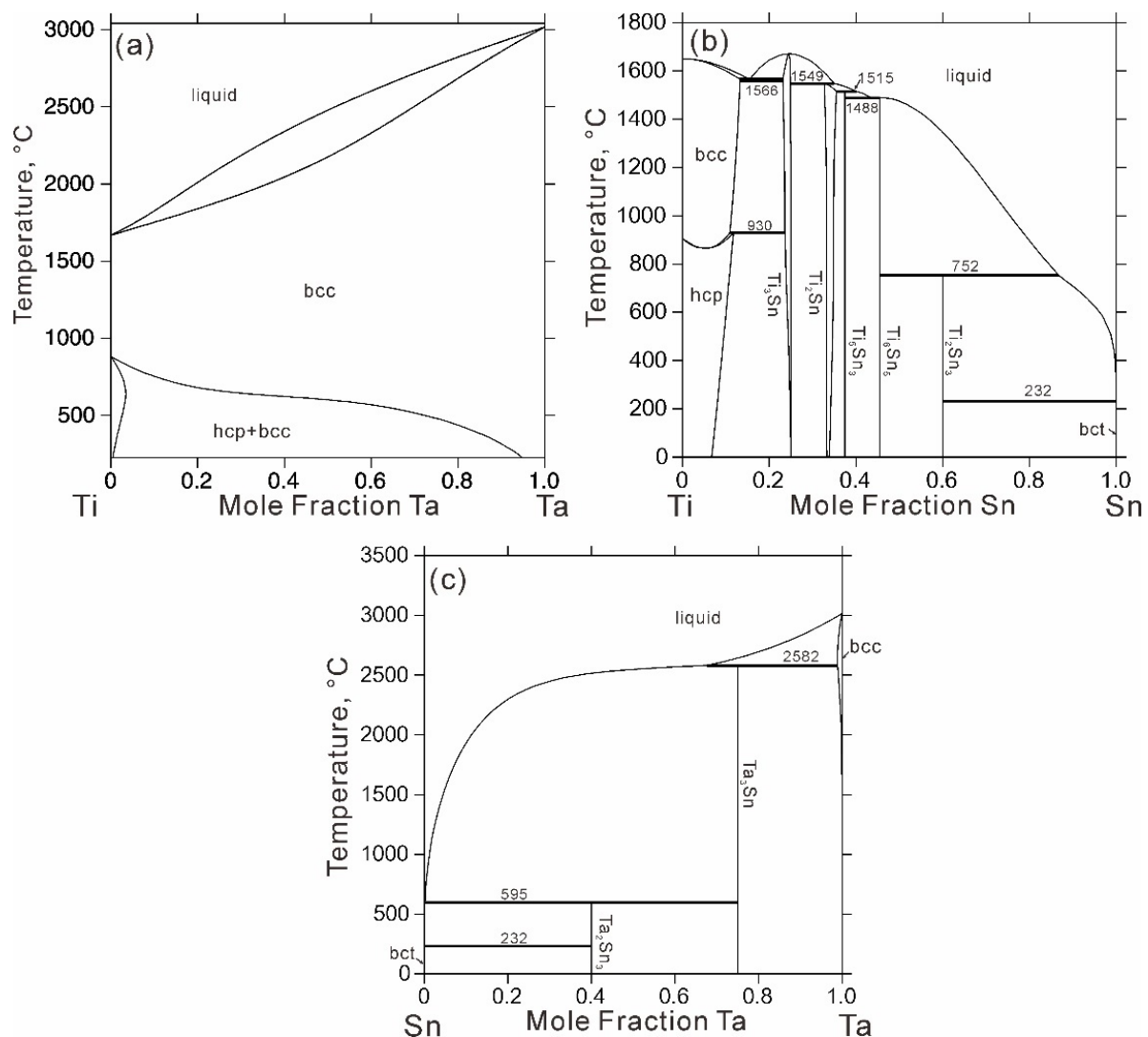


Figure 1. Calculated binary phase diagrams: (a) Ti-Ta data from Ref. [12], (b) Ti-Sn data from Ref. [13] and (c) Ta-Sn data from Ref. [14].

3. Thermodynamic Models

In the present modeling, the Gibbs energy expressions for pure Ti, Ta and Sn are taken from the SGTE compilation by Dinsdale [18]. For the Ti-Ta binary system, the thermodynamic description from Saunders [12] have been have been applied in the development of thermodynamic database for cemented carbides [11,19], which was considered to be reliable and thus adopted in the present work. The first assessment of the Ti-Sn binary system is from the work by Hayes [20]. However, the later detected intermetallic compound, Ti_2Sn_3 , was not considered in that work. Recently, another two reassessments of the Ti-Sn system were reported [13,21], which show no major difference in the reproduction of experimental data. The more recent assessment from Yin et al. [13] performed based on their own experimental data at the Sn-rich side was thus adopted in the present work. To date, there are two assessments for the Ta-Sn binary system in the literature [14,15]. Two intermetallic compounds, Ta_3Sn and Ta_2Sn_3 , were experimentally detected by Basile [22] and were further accepted and used to construct the Ta-Sn phase diagram by Okamoto [23]. However, Ta_2Sn_3 was simply modeled as $TaSn_2$ in the assessment by Marker et al. [15]

in order to keep compatible towards similar systems like V-Sn and Nb-Sn. The treatment of TaSn₂ ignoring its experimental composition seems to be unsuitable, especially when regarding the Ti₂Sn₃ compound in another similar Ti-Sn system. Consequently, the assessment of the Ta-Sn system from Wang et al. [14] was adopted in the present work.

The phases in the Ti-Ta-Sn system were modeled according to compound energy formalism [24]. The present modeling of the Ti-Ta-Sn system was based on the recent evaluations of the Ti-Ta [12], Ti-Sn [13] and Ta-Sn [14] binary systems. The solution phases, liquid, bcc, hcp, and bct, were described by substitutional solution model using the Redlich-Kister polynomial [25]:

$${}^0G_m^\phi = \sum_i x_i {}^0G_i^\phi + RT \sum_i x_i \ln x_i + \sum_{i,j>i} x_i x_j \sum_v {}^vL_{i,j}^\phi (x_i - x_j)^v + {}^{ex}G_m^\phi \quad (1)$$

$${}^{ex}G_m^\phi = x_{Sn} x_{Ta} x_{Ti} (x_{Sn} {}^0L_{Sn,Ta,Ti}^\phi + x_{Ta} {}^1L_{Sn,Ta,Ti}^\phi + x_{Ti} {}^2L_{Sn,Ta,Ti}^\phi) \quad (2)$$

where x_i and x_j represent the molar fractions of elements ($i, j = \text{Sn, Ta, Ti}$). ${}^0G_i^\phi$ is the reference Gibbs energy of pure i at 298 K and 1 bar. ${}^vL_{i,j}^\phi$ is the interaction parameter from binary system. ${}^vL_{Sn,Ta,Ti}^\phi$ ($v = 0, 1, 2$) are ternary interaction parameters to be evaluated in the present work.

According to the sublattice model developed by Hillert and Staffansson [26], a two-sublattice model was employed to describe the intermetallic binary compounds, Ti₃Sn, Ti₂Sn, Ti₅Sn₃, Ti₆Sn₅, Ti₂Sn₃, Ta₃Sn, Ta₂Sn₃, and a three-sublattice model for stoichiometric ternary compound Ti₃₆Ta₂₈Sn₃₆. Taking a phase ϕ modeled by (Sn, Ta, Ti)_a(Sn, Ta, Ti)_c for example, its Gibbs energy can be expressed as follows:

$${}^0G_m^\phi = \sum_i \sum_j y'_i y''_j G_{i,j}^\phi + RT (a \sum_i y'_i \ln y'_i + c \sum_j y''_j \ln y''_j) + {}^{ex}G_m^\phi \quad (3)$$

$${}^{ex}G_m^\phi = \sum_i y'_i \sum_{m,n>m} y''_m y''_n \sum_v {}^vL_{i:m,n}^\phi (y''_m - y''_n)^v + \sum_{i,j>i} y'_i y'_j \sum_m y''_m \sum_v {}^vL_{i,j:m}^\phi (y''_m - y''_n)^v + \sum_{i,j} \sum_{m,n} y'_i y'_j y''_m y''_n L^{rec} \quad (4)$$

where y' and y'' are the site fractions of element in the first and second sublattices. $G_{i,j}^\phi$ indicates the Gibbs energy of a hypothetical state where the first and second sublattices are completely filled by i and j , respectively. The second term of Equation (3) describes the energy contribution due to ideal mixing in each sublattice. L^{rec} represents the reciprocal parameter.

Using Thermo-Calc packages [27], the model parameters were evaluated according to the uncertainty of adopted experimental data and changed by trial and error during the assessment, until most of the selected experimental information can be reproduced within the expected uncertainty limits. The thermodynamic parameters obtained in the present work are listed in Table 2.

Table 2. Summary of the thermodynamic parameters in the Ti–Ta–Sn system [★].

Phase/Model	Thermodynamic Parameters	Reference
Liquid: (Sn,Ta,Ti) ₁	${}^0L_{\text{Sn,Ta}}^{\text{liquid}} = -9735.8 + 17.37T$	[14]
	${}^0L_{\text{Ta,Ti}}^{\text{liquid}} = 1000$	[12]
	${}^1L_{\text{Ta,Ti}}^{\text{liquid}} = -7000$	[12]
	${}^0L_{\text{Sn,Ti}}^{\text{liquid}} = -91,598 - 0.9416T$	[13]
	${}^1L_{\text{Sn,Ti}}^{\text{liquid}} = 45,682 - 12.1045T$	[13]
bcc: (Sn,Ta,Ti) ₁ (Va) ₃	${}^0L_{\text{Sn,Ta:Va}}^{\text{bcc}} = 79,927.2$	[14]
	${}^0L_{\text{Ta,Ti:Va}}^{\text{bcc}} = 12,000$	[12]
	${}^1L_{\text{Ta,Ti:Va}}^{\text{bcc}} = -2500$	[12]
	${}^0L_{\text{Sn,Ti:Va}}^{\text{bcc}} = -142,089 + 28.1423T$	[13]
	${}^1L_{\text{Sn,Ti:Va}}^{\text{bcc}} = 41,211$	[13]
	${}^0L_{\text{Sn,Ta,Ti:Va}}^{\text{bcc}} = -400,000$	This work
hcp: (Sn,Ta,Ti) ₁ (Va) _{0.5}	${}^1L_{\text{Sn,Ta,Ti:Va}}^{\text{bcc}} = -500,000$	This work
	${}^2L_{\text{Sn,Ta,Ti:Va}}^{\text{bcc}} = -150,000$	This work
	${}^0L_{\text{Ta,Ti:Va}}^{\text{hcp}} = 8500$	[12]
	${}^0L_{\text{Sn,Ti:Va}}^{\text{hcp}} = -127,549.6 + 23.2048T$	[13]
bct: (Sn,Ta,Ti) ₁	${}^1L_{\text{Sn,Ti:Va}}^{\text{hcp}} = 64,500.5 + 7.7566T$	[13]
	${}^2L_{\text{Sn,Ti:Va}}^{\text{hcp}} = 31,287.5$	[13]
	${}^0L_{\text{Sn,Ti}}^{\text{bct}} = 50,000$	[13]
Ti ₃ Sn: (Ta,Ti) ₃ (Sn,Va) ₁	${}^0G_{\text{Ti:Sn}}^{\text{Ti}_3\text{Sn}} = -141,133 + 1.1272T + 3\text{GHSERTI} + \text{GHSERSN}$	[13]
	${}^0G_{\text{Ti:Va}}^{\text{Ti}_3\text{Sn}} = 15,000 + 3\text{GHSERTI}$	[13]
	${}^0G_{\text{Ta:Sn}}^{\text{Ti}_3\text{Sn}} = 20,000 + 3\text{GHSERTA} + \text{GHSERSN}$	This work
	${}^0G_{\text{Ta:Va}}^{\text{Ti}_3\text{Sn}} = 15,000 + 3\text{GHSERTA}$	This work
Ti ₂ Sn: (Ta,Ti,Va) ₂ (Sn,Va) ₁	${}^0G_{\text{Ta,Ti:Sn}}^{\text{Ti}_3\text{Sn}} = -113,207 + 65T$	This work
	${}^0G_{\text{Ti:Sn}}^{\text{Ti}_2\text{Sn}} = -122,344 + 6.0034T + 2\text{GHSERTI} + \text{GHSERSN}$	[13]
	${}^0G_{\text{Ti:Va}}^{\text{Ti}_2\text{Sn}} = 10,000 + 2\text{GHSERTI}$	[13]
	${}^0G_{\text{Va:Sn}}^{\text{Ti}_2\text{Sn}} = 5000 + \text{GHSERSN}$	[13]
	${}^0G_{\text{Va:Va}}^{\text{Ti}_2\text{Sn}} = 300,000$	[13]
	${}^0G_{\text{Ti:Sn,Va}}^{\text{Ti}_2\text{Sn}} = -34,085.17$	[13]
	${}^0G_{\text{Ti,Va:Sn}}^{\text{Ti}_2\text{Sn}} = -49,803.91 + 24.471T$	[13]
Ti ₅ Sn ₃ : (Ta,Ti) ₅ (Sn) ₃	${}^0G_{\text{Ta:Sn}}^{\text{Ti}_2\text{Sn}} = 15,000 + 2\text{GHSERTA} + \text{GHSERSN}$	This work
	${}^0G_{\text{Ta:Va}}^{\text{Ti}_2\text{Sn}} = 15,000 + 2\text{GHSERTA}$	This work
	${}^0L_{\text{Ta,Ti:Sn}}^{\text{Ti}_2\text{Sn}} = -145,816 + 80T$	This work
	${}^0G_{\text{Ti:Sn}}^{\text{Ti}_5\text{Sn}_3} = -330,186.45 + 5.3066T + 5\text{GHSERTI} + 3\text{GHSERSN}$	[13]
Ti ₆ Sn ₅ : (Ta,Ti) ₆ (Sn) ₅	${}^0G_{\text{Ta:Sn}}^{\text{Ti}_5\text{Sn}_3} = 40,000 + 5\text{GHSERTA} + 3\text{GHSERSN}$	This work
	${}^0G_{\text{Ta,Ti:Sn}}^{\text{Ti}_5\text{Sn}_3} = -179,785 + 20T$	This work
	${}^0G_{\text{Ti:Sn}}^{\text{Ti}_6\text{Sn}_5} = -468,938.25 + 5.3729T + 6\text{GHSERTI} + 5\text{GHSERSN}$	[13]
Ti ₂ Sn ₃ : (Ta,Ti) ₂ (Sn) ₃	${}^0G_{\text{Ta:Sn}}^{\text{Ti}_6\text{Sn}_5} = 55,000 + 6\text{GHSERTA} + 5\text{GHSERSN}$	This work
	${}^0L_{\text{Ta,Ti:Sn}}^{\text{Ti}_6\text{Sn}_5} = -300,774$	This work
	${}^0G_{\text{Ti:Sn}}^{\text{Ti}_2\text{Sn}_3} = -173,931.7 + 7.82593T + 2\text{GHSERTI} + 3\text{GHSERSN}$	[13]
Ta ₃ Sn: (Ta,Ti) ₃ (Sn) ₁	${}^0G_{\text{Ta:Sn}}^{\text{Ti}_2\text{Sn}_3} = -25,000 + 2\text{GHSERTA} + 3\text{GHSERSN}$	This work
	${}^0G_{\text{Ta,Ti:Sn}}^{\text{Ti}_2\text{Sn}_3} = -48,000$	This work
	${}^0G_{\text{Ta:Sn}}^{\text{Ta}_3\text{Sn}} = -67,693.3 + 9.077T + 3\text{GHSERTA} + \text{GHSERSN}$	[14]
Ta ₂ Sn ₃ : (Ta) ₂ (Sn) ₃	${}^0G_{\text{Ti:Sn}}^{\text{Ta}_3\text{Sn}} = 20,000 + 3\text{GHSERTI} + \text{GHSERSN}$	This work
	${}^0G_{\text{Ta,Ti:Sn}}^{\text{Ta}_3\text{Sn}} = -184,472$	This work
Ti ₃₆ Ta ₂₈ Sn ₃₆ : (Ti) _{0.36} (Ta) _{0.28} (Sn) _{0.36}	${}^0G_{\text{Ta:Sn}}^{\text{Ta}_2\text{Sn}_3} = -77,332.2 + 29.6428T + 2\text{GHSERTA} + 3\text{GHSERSN}$	[14]
	${}^0G_{\text{Ti:Ta:Sn}}^{\text{Ti}_{36}\text{Ta}_{28}\text{Sn}_{36}} = -22,135.2 - 10T + 0.36\text{GHSERTI} + 0.28\text{GHSERTA} + 0.36\text{GHSERSN}$	This work

[★] All parameters are given in J/(mole of atoms); Temperature (T) in K. The Gibbs energies for the pure elements are taken from the compilation of Dinsdale [18]. GHSERXX (XX = SN, TA and TI) are the reference state of Gibbs energies.

4. Results and Discussion

Figures 2 and 3 show the calculated isothermal sections of the Ti-Ta-Sn system at 973 and 1173 K compared with experimental information [16,17], respectively. The chemical compositions of the annealed alloys together with the corresponding equilibrium phases are displayed in the figures. Due to small solid solubility or limited experimental verification, ternary solid solubility only considering the substitution between Ti and Ta was employed to describe intermetallic compounds, except Ti_3Sn and Ti_2Sn . Table 3 shows the calculated solubilities of the third element in binary compounds compared with experimental data [16,17]. As can be seen, the experimentally determined results can be well reproduced by the present calculations with the consideration of experiment errors.

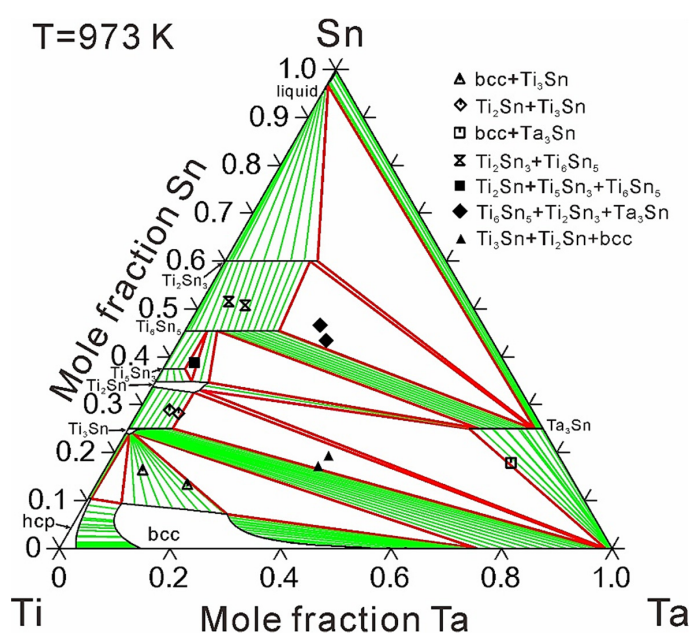


Figure 2. Calculated isothermal section of the Ti-Ta-Sn ternary system at 973 K, compared with experimental data [16].

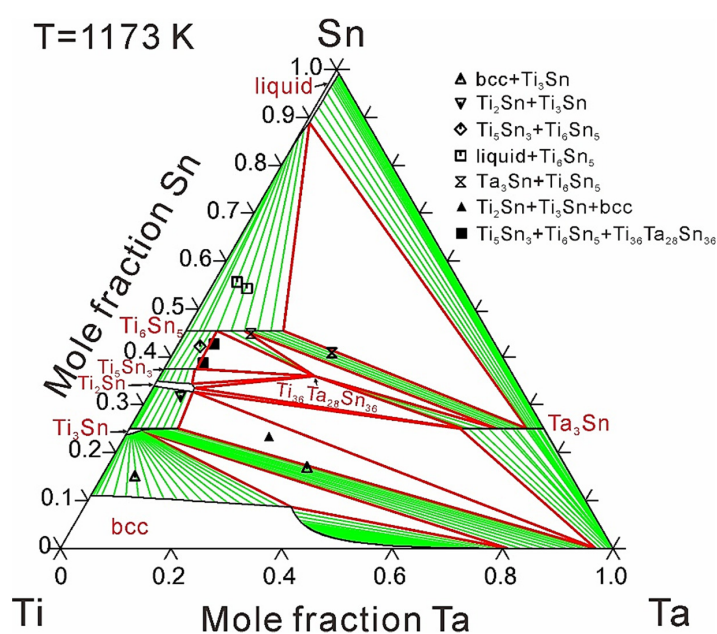


Figure 3. Calculated isothermal section of the Ti-Ta-Sn ternary system at 1173 K, compared with experimental data [17].

A total of four two-phase regions and three three-phase regions at 973 K, and five two-phase regions and two three-phase regions at 1173 K have been experimentally detected by Wang et al. [16,17], signed by vacant symbols for two-phase regions and solid symbols for three-phase regions in Figures 2 and 3. As can be seen in Figures 2 and 3, all the three-phase regions and most of the two-phase regions can be well reproduced based on the present thermodynamic modeling. As can be seen, a miscibility gap occurs in the bcc phase. The ternary solid solubility of bcc phase is large at Ti-rich region while rare at Nb-rich region, almost no Sn solubility at the compositions near 50 at.% Ta at 973 K and 65 at.% Ta at 1173 K. This phenomenon may be caused by the over-stability of bcc phase at the Ti-Ta boundary near the Ta corner. Any attempt to enlarge the ternary solubility of the bcc phase near the Ta corner would cause unreasonable miscibility gap of bcc phase far away from the Ti-Ta boundary. As a result, the experimental data about several two-phase regions concerning the bcc phase were given a small weight during the optimization process in order to achieve a general satisfaction. According to the experimental data, the ternary compound, $Ti_{36}Ta_{28}Sn_{36}$, is stable at 1173 K, while disappears at 973 K. As can be seen, the thermal stabilities of $Ti_{36}Ta_{28}Sn_{36}$ can be well reproduced by using the present thermodynamic modeling.

Table 3. Solubilities of the third element in binary compounds.

Compounds	Temperature, K	Solubilities of the Third Element, at. %		Reference
		Ti	Ta	
Ti_3Sn	973	-	8.3	[16]
		-	8.0	This work
	1173	-	9.3	[17]
Ti_2Sn	973	-	9.0	This work
		-	over 8.8	[16]
	1173	-	9.7	This work
Ti_5Sn_3	973	-	over 7.3	[17]
		-	7.6	This work
	1173	-	4.2	[16]
Ti_6Sn_5	973	-	4.0	This work
		-	6.1	[17]
	1173	-	6.0	This work
Ta_3Sn	973	-	16.8	[16]
		-	17.0	This work
	1173	-	over 15.5	[17]
Ta_3Sn	973	21.3	17.6	This work
		20.8	over 10.9	[16]
	1173	24.9	11.6	This work
		25.3	over 8.8	[17]
			15.2	This work

On the basis of the presently obtained thermodynamic description of the Ti-Ta-Sn system, the liquidus projection appended with isothermal lines is shown in Figure 4. Figure 4b presents an enlarged region in order to display the complicate reactions near the Ti-Sn boundary, 0 to 5 at.% Ta. The invariant reactions on the liquidus surface are listed in Table 4. As can be seen in Figure 4, for a Ti-Sn alloy, the bcc primary phase region can be significantly enlarged from 16 at.% Sn up to a maximum 30 at.% Sn by doping about 1.5 at.% Ta. Further increasing the content of Ta, the bcc primary phase region shrinks gradually. When doping a large amount of Ta and Sn in Ti-based alloys, $Ti_{36}Ta_{28}Sn_{36}$ may precipitate as the primary phase instead of bcc phase, which would strongly influence the properties of Ti-based alloys.

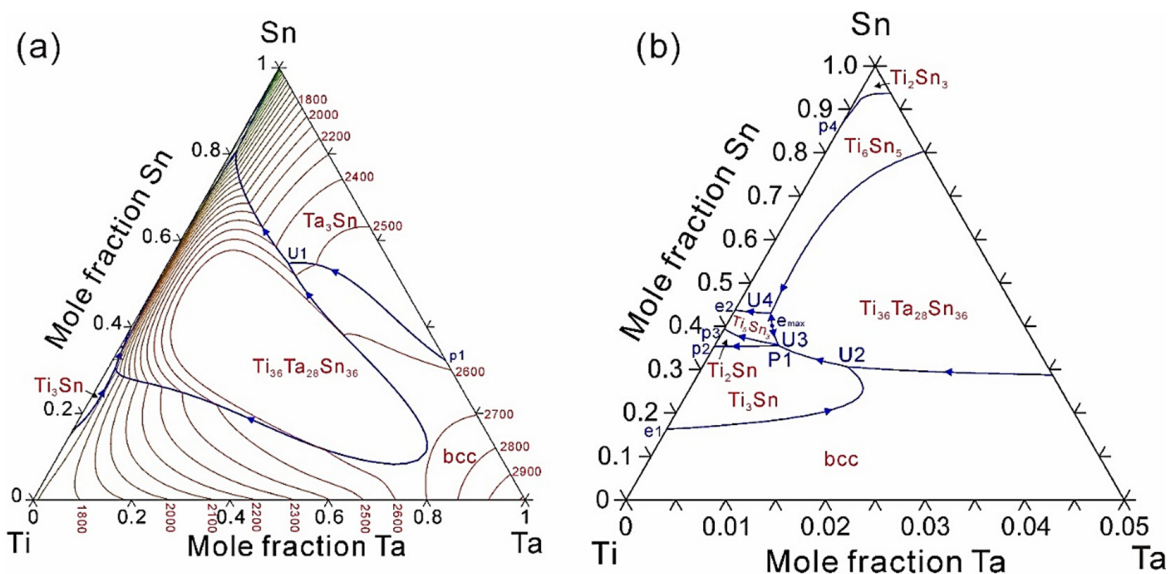


Figure 4. (a,b) Calculated liquidus projection of the Ti-Ta-Sn ternary system.

Table 4. Calculated the invariant reactions on the liquidus surface in the Ti-Ta-Sn system.

Type	Invariant Reaction	Temperature, °C	Source
p1	liquid + bcc = Ta ₃ Sn	2582	[14]
U ₁	liquid + bcc = Ta ₃ Sn + Ti ₃₆ Ta ₂₈ Sn ₃₆	2450	This work
U ₂	liquid + bcc = Ti ₃ Sn + Ti ₃₆ Ta ₂₈ Sn ₃₆	1628	This work
e1	liquid = bcc + Ti ₃ Sn	1566	[13]
p2	liquid + Ti ₃ Sn = Ti ₂ Sn	1549	[13]
P2	liquid + Ti ₃ Sn + Ti ₃₆ Ta ₂₈ Sn ₃₆ = Ti ₂ Sn	1542	This work
U3	liquid + Ti ₃₆ Ta ₂₈ Sn ₃₆ = Ti ₂ Sn + Ti ₅ Sn ₃	1541	This work
U4	liquid + Ti ₃₆ Ta ₂₈ Sn ₃₆ = Ti ₆ Sn ₅ + Ti ₅ Sn ₃	1519	This work
p3	liquid + Ti ₂ Sn = Ti ₅ Sn ₃	1515	[13]
e2	liquid = Ti ₅ Sn ₃ + Ti ₆ Sn ₅	1488	[13]
p4	liquid + Ti ₆ Sn ₅ = Ti ₂ Sn ₃	752	[13]

Commonly, Ti based alloys undergo aging treatment after cooling in order to precipitate $\alpha_{\text{hcp-Ti}}$ phase in $\beta_{\text{bcc-(Ti,Ta)}}$, which is an effective way to improve the mechanical properties. Consequently, it is interesting and technically important to know when the transformation from $\beta_{\text{bcc-(Ti,Ta)}}$ to $\alpha_{\text{hcp-Ti}}$ takes place and how the alloying element influences the transformation. Figure 5 shows the influence of Ta and Sn content on the precipitation temperature and amount of $\alpha_{\text{hcp-Ti}}$ phase in $\beta_{\text{bcc-(Ti,Ta)}}$ phase. According to the calculations, it is obvious that increasing the contents of Ta and Sn, especially Ta content, can significantly decrease the transformation temperature. Besides, when aging at 600 °C, the increase in Ta content may reduce the amount of $\alpha_{\text{hcp-Ti}}$ precipitates, while the influence of Sn content is negligible. Thus, prior to experiment, the alloying composition and aging heat treatment schedule can be designed and optimized based on thermodynamic calculations to further obtain optimal properties.

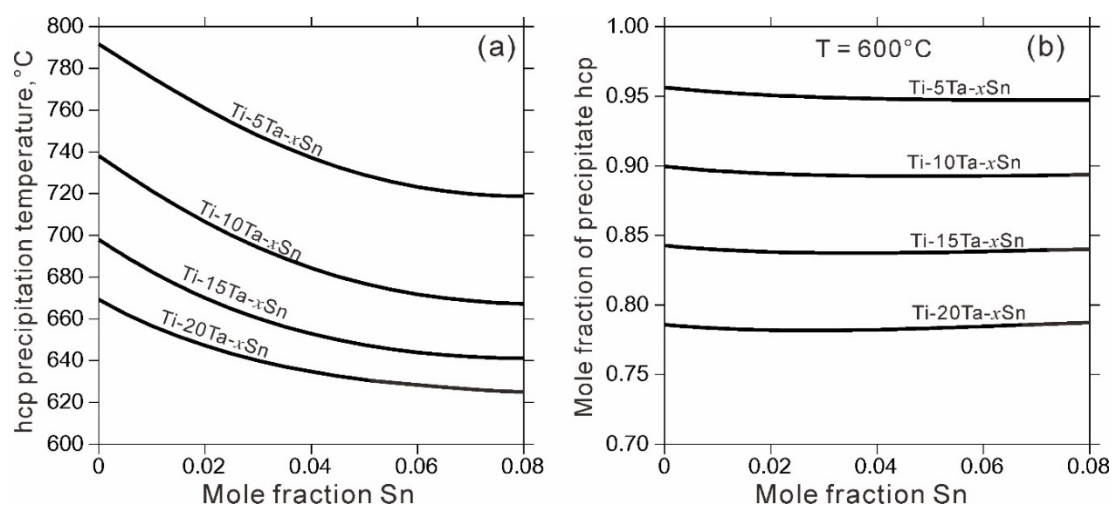


Figure 5. Influence of Ta and Sn contents (at.%) on the precipitation temperature (a) and amount (b) of α -hcp-Ti phase in β -bcc-(Ti,Ta) phase.

Recently, Ti-based alloys mainly with the contents of Ta and Sn between 10 and 30 at.% have attracted more and more attentions due to their favorable properties [3,7,28]. Based on the presently obtained thermodynamic description of the Ti-Ta-Sn system, the Scheil solidification simulations of Ti-20Ta- x Sn ($x = 5, 15$ and 25) as-cast alloys were performed, as shown in Figure 6. The Scheil solidification curves can provide various information like primary phase, transformation temperature, solidification path and so on. For a Ti-20Ta alloy, when the content of alloying element Sn is less than 25 at.%, the primary phase would be β -bcc-(Ti,Ta) phase. While increasing Sn content up to 25 at.%, the primary phase changes to be $\text{Ti}_{36}\text{Ta}_{28}\text{Sn}_{36}$. Moreover, large Sn content (exceeding 15 at.%) leads to the formation of Ti_3Sn and Ti_6Sn_5 . As can be seen, performing Scheil solidification simulations based on the presently obtained thermodynamic description of the Ti-Ta-Sn system can predict the primary phase and solidified phases in the as-cast alloys, which may affect the subsequent microstructure and properties.

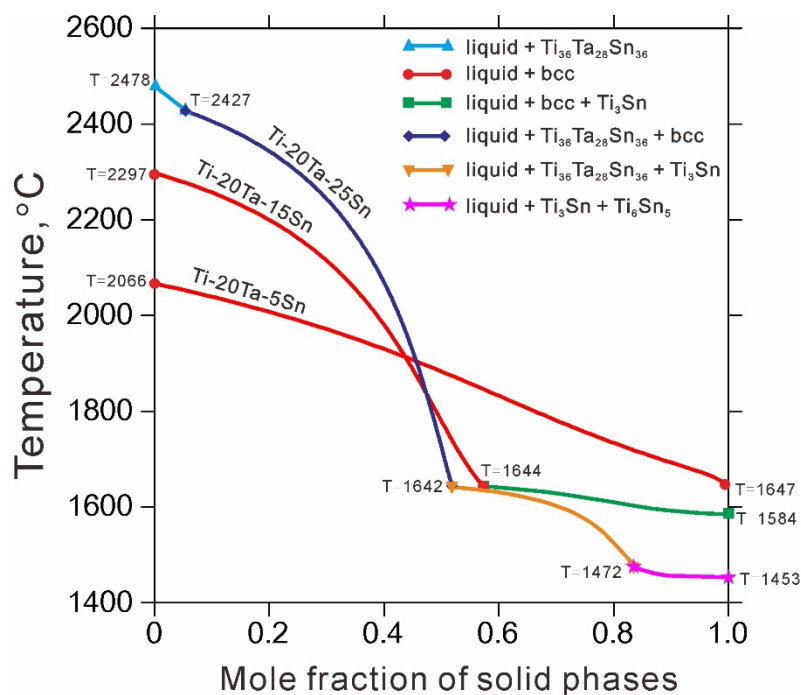


Figure 6. Scheil solidification simulations of Ti-20Ta- x Sn ($x = 5, 15$ and 25) (at.%) as-cast alloys.

5. Conclusions

The phase equilibrium data in the Ti-Ta-Sn system have been critically reviewed. A thermodynamic modeling of the Ti-Ta-Sn system has been performed based on reliable experimental data. Comparisons between experimental and calculated isothermal sections at 973 and 1173 K show that most of the experimental data can be well accounted for by the present thermodynamic description. Based on thermodynamic calculations, the influence of the content of alloying elements Ta and Sn on the precipitation temperature and amount of α -hcp-Ti in β -bcc-(Ti,Ta) and the microstructures of as-cast alloys have been studied, which provides an effective way to design Ti based alloys with high performances.

Author Contributions: Conceptualization, Y.P. and L.Y. (Lifang Yan); methodology, Y.P. and L.Y. (Lifang Yan); validation, T.L., and L.Y. (Lifang Yan); formal analysis, Y.P.; investigation, L.Y. (Lifang Yan), L.Y. (Lianwu Yan) and S.H.; resources, T.L.; data curation, T.L.; writing—original draft preparation, Y.P.; writing—review and editing, L.Y. (Lifang Yan) and T.X.; visualization, S.H. and T.X.; supervision, T.X.; project administration, Y.P. and S.H.; funding acquisition, Y.P., T.X. and S.H. All authors have read and agreed to the published version of the manuscript.

Funding: The financial support from Natural Science Foundation of Hunan Province of China (No. 2020JJ6077, 2020JJ6069), Key Research and Development Program of Hunan Province (No. 2019GK2052), Science Challenge Project of China (Grant No. TZ2016004) and Major Science and Technology Innovation Projects of Shandong Key Research and Development Plan (No. 2019JZZY010361), Key Scientific Research Projects of Hunan Province Education Department (No. 20A147), and Constructing the Special Project of Science Popularization in Hunan Province (2020ZK4023) is acknowledged.

Institutional Review Board Statement: Not applicable.

Informed Consent Statement: Not applicable.

Data Availability Statement: Data sharing is not applicable for this article.

Conflicts of Interest: The authors declare no conflict of interest.

References

1. Banerjee, D.; Williams, J.C. Perspectives on Titanium Science and Technology. *Acta Mater.* **2013**, *61*, 844–879. [[CrossRef](#)]
2. Yoshimitsu, O.; Katsuda, S. Biological Safety Evaluation and Surface Modification of Biocompatible Ti–15Zr–4Nb Alloy. *Materials* **2021**, *14*, 731.
3. Kim, H.Y.; Fukushima, T.; Buenconsejo, P.J.S.; Nam, T.H.; Miyazaki, S. Martensitic transformation and shape memory properties of Ti-Ta-Sn high temperature shape memory alloys. *Mater. Sci. Eng. A* **2011**, *528*, 7238–7246. [[CrossRef](#)]
4. Biesiekierski, A.; Wang, J.; Gepreel, M.A.; Wen, C. A new look at biomedical Ti-based shape memory alloys. *Acta Biomater.* **2012**, *8*, 1661–1669. [[CrossRef](#)] [[PubMed](#)]
5. Panicker, A.G.; Acharya, S.; Laxmi, D.V.; Suwas, S.; Chatterjee, K. Study of the influence of Zr on the mechanical properties and functional response of Ti-Nb-Ta-Zr-O alloy for orthopedic applications. *Mater. Des.* **2019**, *164*, 107555.
6. Li, M.J.; Min, X.H.; Yao, K.; Ye, F. Novel insight into the formation of α'' -martensite and ω -phase with cluster structure in metastable Ti-Mo alloys. *Acta Mater.* **2019**, *164*, 332–333. [[CrossRef](#)]
7. Tong, Y.X.; Guo, B.; Zheng, Y.F.; Chung, C.Y.; Ma, L.W. Effects of Sn and Zr on the microstructure and mechanical properties of Ti-Ta-based shape memory alloys. *J. Mater. Eng. Perform.* **2011**, *20*, 762–766. [[CrossRef](#)]
8. Guo, B.; Tong, Y.X.; Chen, F.; Zheng, Y.F.; Li, L.; Chung, C.Y. Effect of Sn addition on the corrosion behavior of Ti-Ta alloy. *Mater. Corros.* **2012**, *63*, 259–263. [[CrossRef](#)]
9. Cremasco, A.; Andrade, P.N.; Contieri, R.J.; Lopes, E.S.N.; Afonso, C.R.M.; Caram, R. Correlations between aging heat treatment, ω phase precipitation and mechanical properties of a cast Ti-Nb alloy. *Mater. Des.* **2011**, *32*, 2387–2390. [[CrossRef](#)]
10. Tag, X.; Ahmed, T.; Rack, H.J. Phase transformations in Ti–Nb–Ta and Ti–Nb–Ta–Zr alloys. *J. Mater. Sci.* **2000**, *35*, 1805–1811.
11. Peng, Y.B.; Du, Y.; Zhou, P.; Zhang, W.B.; Chen, W.M.; Chen, L.; Wang, S.Q.; Wen, G.H.; Xie, W. CSUTDCC1—A thermodynamic database for multicomponent cemented carbides. *Int. J. Refract. Met. Hard Mater.* **2014**, *42*, 57–70. [[CrossRef](#)]
12. Saunders, N. System Ta-Ti. In *Thermochemical Database for Light Metal Alloys*; Ansara, I., Dinsdale, A.T., Rand, M.H., Eds.; Office for Official Publications of the European Communities: Luxembourg, 1998; Volume 2, pp. 293–296.
13. Liu, C.; Klotz, U.E.; Uggowitzer, P.J.; Löffler, J.F. Thermodynamic assessment of the Sn-Ti system. *Monatsh. Chem.* **2005**, *136*, 1921–1930. [[CrossRef](#)]
14. Wang, J.; Tuo, B.; Hu, X.; Liu, Z. Thermodynamic properties and thermodynamic assessment of Ta-Sn system. *Adv. Mater. Res.* **2013**, *821*, 848–853. [[CrossRef](#)]

15. Marker, C.; Shang, S.; Liu, X.L.; Lindwall, G.; Liu, Z.-K. First-principles calculations and thermodynamic modeling of the Sn-Ta system. *CALPHAD* **2017**, *57*, 46–54. [[CrossRef](#)]
16. Wang, J. Study on Phase Diagrams, Thermodynamics of Phase Equilibria and Alloy Design of Titanium Alloys. Ph.D. Thesis, Central South University, Changsha, China, 2015.
17. Wang, J.; Liu, L.; Zhang, X.; Wang, X.; Bai, W. Isothermal section of the Ti-Ta-Sn ternary system at 1173 K. *J. Phase Equilib. Diff.* **2014**, *39*, 273–280. [[CrossRef](#)]
18. Dinsdale, A.T. SGTE data for pure elements. *CALPHAD* **1991**, *15*, 317–425. [[CrossRef](#)]
19. Peng, Y.; Zhou, P.; Du, Y.; Chang, K. Thermodynamic evaluation of the C-Ta-Ti system and extrapolation to the C-Ta-Ti-N system. *Int. J. Refract. Met. Hard Mater.* **2013**, *40*, 36–42. [[CrossRef](#)]
20. Hayes, F. System Sn-Ti. In *Thermochemical Database for Light Metal Alloys*; Ansara, I., Dinsdale, A.T., Rand, M.H., Eds.; Office for Official Publications of the European Communities: Luxembourg, 1998; Volume 2, pp. 284–290.
21. Yin, F.; Tedenac, J.C.; Gascoin, F. Thermodynamic modelling of the Ti-Sn system and calculation of the Co-Ti-Sn system. *CALPHAD* **2007**, *31*, 370–379. [[CrossRef](#)]
22. Basile, F. Crystallographic study and supraconductive properties of compounds V_3Sn and Ta_2Sn_3 . *Ann. Chim.* **1971**, *6*, 241–244.
23. Okamoto, H. Sn-Ta (Tin-Tantalum) system. *J. Phase Equilibria* **2003**, *24*, 484. [[CrossRef](#)]
24. Andersson, J.O.; Guillermet, A.F.; Hillert, M.; Jansson, B.; Sundman, B. A compound-energy model of ordering in a phase with sites of different coordination numbers. *Acta Metall.* **1986**, *34*, 437–445. [[CrossRef](#)]
25. Redlich, O.; Kister, A.T. Algebraic representation of thermodynamic properties and the classification of solutions. *Ind. Eng. Chem.* **1948**, *40*, 345–348. [[CrossRef](#)]
26. Hillert, M.; Staffansson, L.I. The regular solution model for stoichiometric phases and ionic melts. *Acta Chem. Scand.* **1970**, *24*, 3618–3626. [[CrossRef](#)]
27. Sundman, B.; Jansson, B.; Andersson, J.O. The Thermo-Calc databank system. *CALPHAD* **1985**, *9*, 153–190. [[CrossRef](#)]
28. Aguilar, C.; Aguirre, T.; Martínez, C.; Barbieri, F.D.; Martín, F.S.; Salinas, V.; Alfonso, I. Improving the mechanical strength of ternary beta titanium alloy (Ti-Ta-Sn) foams using a bimodal microstructure. *Mater. Des.* **2020**, *195*, 108945. [[CrossRef](#)]